Finite Element Digital Image Correlation for Cardiac Strain Analysis from 3D Whole-Heart Tagging

Martin Genet, Christian T Stoeck, Constantin von Deuster, Lik Chuan Lee, Julius Guccione, Sebastian Kozerke

Title
Finite Element Digital Image Correlation for Cardiac Strain Analysis from 3D Whole-Heart Tagging

Authors
Martin Genet, Christian T. Stoeck, Constantin von Deuster, Lik Chuan Lee, Julius M. Guccione, Sebastian Kozerke

Abstract (max 750 words)
Introduction
Whole-heart 3D CSPAMM allows for fast and reliable functional imaging of the beating heart by mapping the deformation of magnetization patterns throughout the left ventricle and cardiac cycle [1]. Its clinical use has been limited mainly due to *(i)* the time-consuming post-processing of tagged MR images, and *(ii)* derivation of clinically relevant biomarkers from the data. Regarding the post-processing of tagged MR images, multiple approaches have been proposed [2]; however, some of these methods are computationally expensive and consensus about a preferred algorithm is still lacking. Regarding clinically relevant prognostic information, biomechanical models are increasingly considered as a potential tool to characterize patient condition and predict patient outcome through the integration of patient-specific data including ventricular strain [3]–[5]; however, the integration of finite element biomechanical models and image data remains challenging.

The objective of the present work was to develop, validate and analyze a finite element digital image correlation tool to extract ventricular strain data from MR images, which can be applied to both 3D CSPAMM images and conventional multi-slice cine images.

Methods
Whole-heart 3D CSPAMM and standard multi-slice cine data were acquired in healthy volunteers on a clinical 1.5T scanner (Philips Achieva, Best, The Netherlands). Imaging parameters for 3D CSPAMM were: spatial resolution 3.5×7.7×7.7mm^3 reconstructed to 1×1×1mm^3, temporal resolution 28ms, tagging distance 7mm. Image acquisition was performed during respiratory navigator gated breathholding. Geometrical stack alignment of all tagged volume images was performed by incorporating navigator offsets and rigid image registration. Multi-slice balanced SSFP cine images were acquired with a spatial resolution of 1.2x1.2x8mm^3 and a temporal resolution of 70ms. Both 3D CSPAMM and cine images were interpolated in time using a Lanczos filter in MeVisLab (MeVis Medical Solutions AG, Bremen, Germany) to yield ca. 50 frames/cycles. Cine images were spatially interpolated as well, still using MeVisLab Lanczos filter, in order to obtain ca. isotropic voxel sizes. Upon manually segmenting the left ventricle on 3D CSPAMM and cine images using MeVisLab, reference left ventricular finite element meshes at end-diastole were generated using GMSH [6] (Figure 1).

The finite element digital image correlation tool used here is based on the hyperelastic warping FEBio [7] plugin, which implements the method described in [8], [9]. Briefly, considering a moving image M, a target image T, and a triangulation of an object on the moving image Ω, the method consists of finding the displacement field $\underline{U}$ that minimizes the functional

$$J(\underline{U}) = \int_\Omega \frac{k}{2}\left(M(\underline{X}) - T(\underline{X}+\underline{U})\right)^2 d\Omega + \int_\Omega \psi(\underline{U})(\underline{X}) d\Omega$$

where k denotes a penalty coefficient, the first term being a similarity term, and ψ the hyperelastic strain energy potential, so that the mechanical energy acts as a regularization term. In the present work, a simple Neo-Hookean potential with unit stiffness is assumed, thus k is the only parameter of the method. For a time

sequence of images, successive images are registered and the successive displacement fields are combined so as to map the motion of the reference mesh.

Optimal penalty factors were determined for cine and 3D CSPAMM images by computing peak circumferential, longitudinal and circumferential-longitudinal strains over a wide range of penalties, and recording the penalty that corresponds to a converged average strain and minimal standard deviation. The strain computation was then validated against a validated implantation of the SinMod method [10] within 3DTagTrack (Gyortools LLC, Zurich, Switzerland). Furthermore, strain data was obtained from cine and 3D CSPAMM images and compared. Finally, the sensitivity of the method to image/mesh misregistration was investigated by manually shifting the reference mesh before applying the warping algorithm.

Results

Optimal penalty factors were identified as 16 for cine images, and 0.5 for 3D CSPAMM (Figure 2).

The proposed method provided similar circumferential strain data compared to the validated SinMod method (Figure 3). Reduced variation of circumferential strain indicates more reliable tracking of the proposed method relative to SinMod.

Global circumferential and longitudinal strain components extracted from cine were found to be similar to strain data extracted from 3D CSPAMM images; however, the circumferential-longitudinal strain component, i.e., the ventricular twist, was not captured appropriately from cine images due to the lack of contrast within the myocardial wall (Figure 4).

Strain extraction from 3D CSPAMM images was found to be much less sensitive to misregistration compared to cine (Figure 5), due to the smoothing of the boundaries in 3D CSPAMM images.

Discussion

Finite element digital image correlation is a promising approach to derive strain data from whole-heart 3D tagging data. In contrast to strain mapping from cine images, image correlation on 3D tagging data captures ventricular twist in agreement with physiological values, and is less sensitive to image misregistration. Accordingly, the method may be more appropriate compared to cine-based strain analysis as reported previously [11], especially when non homogeneous strain fields are expected, for instance in infarcted hearts, and for which intra-ventricular wall contrast is necessary.

Acknowledgment

This work was supported by a Marie-Curie international outgoing fellowship within the 7th European Community Framework Program (MG); UK EPSRC grant EP/I018700/1 (CTS, CVD, SK); NIH grants R01-HL-077921, R01-HL-118627, and U01-HL-119578 (JMG).

References

[1] A. K. Rutz, S. Ryf, S. Plein, P. Boesiger, and S. Kozerke, “Accelerated whole-heart 3D CSPAMM for myocardial motion quantification.,” *Magn. Reson. Med.*, vol. 59, no. 4, pp. 755–63, Apr. 2008.

[2] C. Tobon-Gomez, M. De Craene, K. McLeod, L. Tautz, W. Shi, A. Hennemuth, A. Prakosa, H. Wang, G. S. Carr-White, S. Kapetanakis, A. Lutz, V. Rasche, T. Schaeffter, C. Butakoff, O. Friman, T. Mansi, M. Sermesant, X. Zhuang, S. Ourselin, H.-O. H.-O. Peitgen, X. Pennec, R. Razavi, D. Rueckert, A. F. F. Frangi, and K. S. K. S. Rhode, “Benchmarking framework for myocardial tracking and deformation algorithms: An open access database,” *Med. Image Anal.*, vol. 17, no. 6, pp. 632–648, Aug. 2013.

[3] L. C. Lee, M. Genet, A. B. Dang, L. Ge, J. M. Guccione, and M. B. Ratcliffe, "Applications of computational modeling in cardiac surgery.," *J. Card. Surg.*, vol. 29, no. 3, pp. 293–302, May 2014.

[4] M. Genet, L. C. Lee, R. Nguyen, H. Haraldsson, G. Acevedo-Bolton, Z. Zhang, L. Ge, K. Ordovas, S. Kozerke, J. M. Guccione, D. A. Saloner, S. Kozerke, and J. M. Guccione, "Distribution of normal human left ventricular myofiber stress at end-diastole and end-systole–a target for in silico studies of cardiac procedures," *J. Appl. Physiol.*, vol. 117, pp. 142–52, 2014.

[5] M. Genet, L. C. Lee, L. Ge, G. Acevedo-Bolton, N. Jeung, A. J. Martin, N. Cambronero, A. Boyle, Y. Yeghiazarians, S. Kozerke, and J. M. Guccione, "A Novel Method for Quantifying Smooth Regional Variations in Myocardial Contractility Within an Infarcted Human Left Ventricle Based on Delay-Enhanced Magnetic Resonance Imaging," *J. Biomech. Eng.*, vol. 137, no. 8, Aug. 2015.

[6] C. Geuzaine and J.-F. Remacle, "Gmsh: a three-dimensional finite element mesh generator with built-in pre- and post-processing facilities," *Int. J. Numer. Methods Eng.*, vol. 79, no. 11, pp. 1309–1331, Sep. 2009.

[7] S. a. Maas, B. J. Ellis, G. a. Ateshian, and J. a. Weiss, "FEBio: Finite Elements for Biomechanics," *J. Biomech. Eng.*, vol. 134, no. 1, p. 011005, 2012.

[8] A. I. Veress, G. T. Gullberg, and J. A. Weiss, "Measurement of Strain in the Left Ventricle during Diastole with cine-MRI and Deformable Image Registration," *J. Biomech. Eng.*, vol. 127, no. 7, p. 1195, Jul. 2005.

[9] N. S. Phatak, S. A. Maas, A. I. Veress, N. a Pack, E. V. R. Di Bella, and J. A. Weiss, "Strain measurement in the left ventricle during systole with deformable image registration," *Med. Image Anal.*, vol. 13, no. 2, pp. 354–61, Apr. 2009.

[10] H. Wang, C. T. Stoeck, S. Kozerke, and A. A. Amini, "Analysis of 3D cardiac deformations with 3D SinMod.," *Conf. Proc. ... Annu. Int. Conf. IEEE Eng. Med. Biol. Soc. IEEE Eng. Med. Biol. Soc. Annu. Conf.*, vol. 2013, pp. 4386–9, Jan. 2013.

[11] W. E. Moody, R. J. Taylor, N. C. Edwards, C. D. Chue, F. Umar, T. J. Taylor, C. J. Ferro, A. A. Young, J. N. Townend, F. Leyva, and R. P. Steeds, "Comparison of magnetic resonance feature tracking for systolic and diastolic strain and strain rate calculation with spatial modulation of magnetization imaging analysis.," *J. Magn. Reson. Imaging*, 2014.

Figures

Figure 1

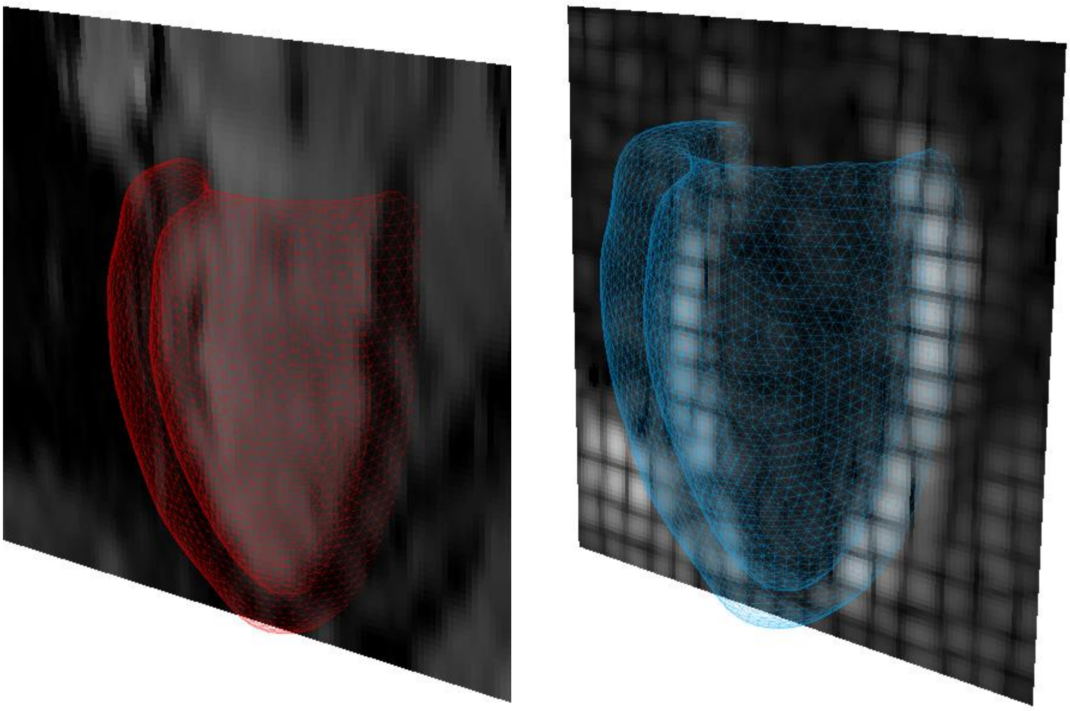

Cine (left) and 3D CSPAMM (right) images with superimposed finite element meshes. The meshes are generated in GMSH, after manual segmentation of the endocardium and epicardium in MeVisLab. They are then used as a support for the displacement field between successive image frames.

Figure 2

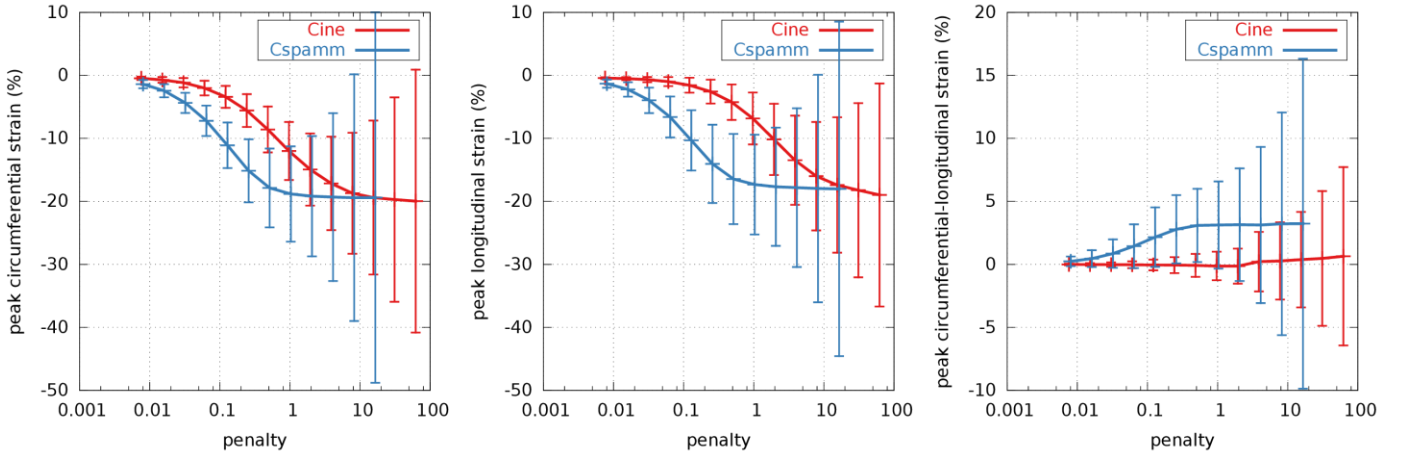

Convergence of the registration method with regard to the penalty coefficient: mean±standard deviation over the entire ventricle of the peak circumferential (left), longitudinal (center) and circumferential-longitudinal (right) strain components, for cine (red) and 3D CSPAMM (blue) image series.

Figure 3

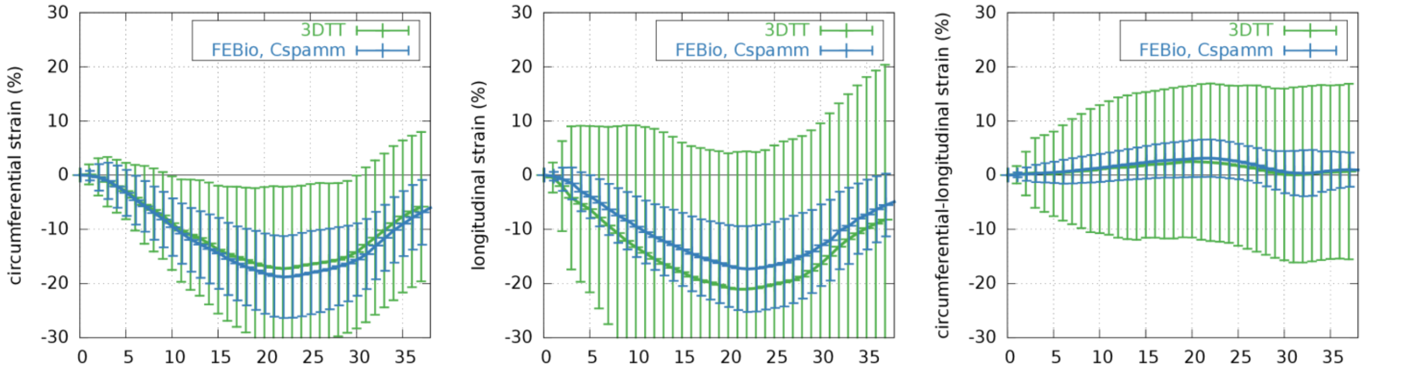

Validation of the method: comparison of time courses of mean±standard deviation over the entire ventricle of circumferential (left), longitudinal (center) and circumferential-longitudinal (right) strain components derived from 3D CSPAMM images (blue) vs. using validated 3DTagTrack software [10] on the mesh points (green).

Figure 4

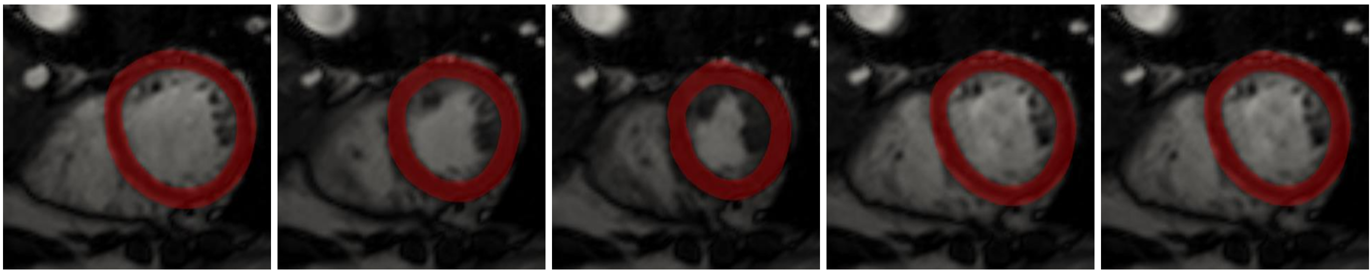

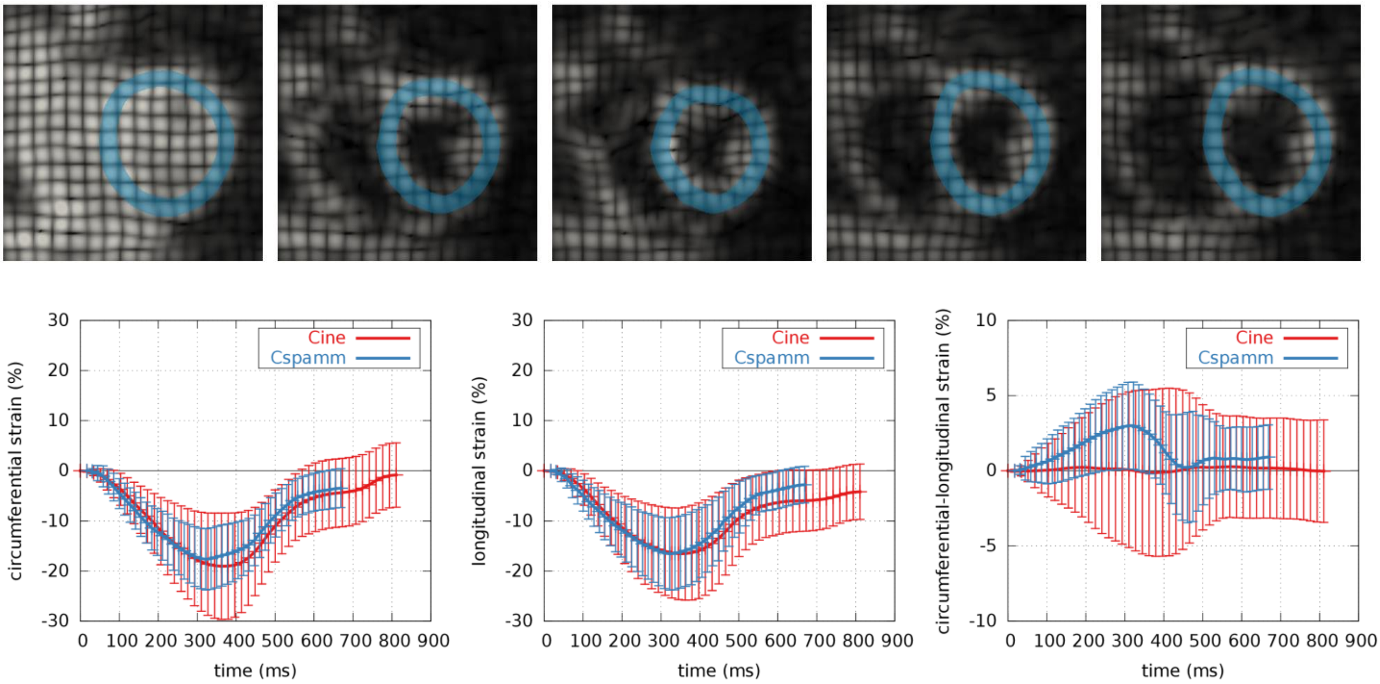

Comparison of times courses of cine (top) and 3D CSPAMM (middle) images with superimposed slices of warped finite element meshes. The bottom line shows comparison of time courses of mean±standard deviation over the entire ventricle of circumferential (left), longitudinal (center) and circumferential-longitudinal (right) strain components.

Figure 5

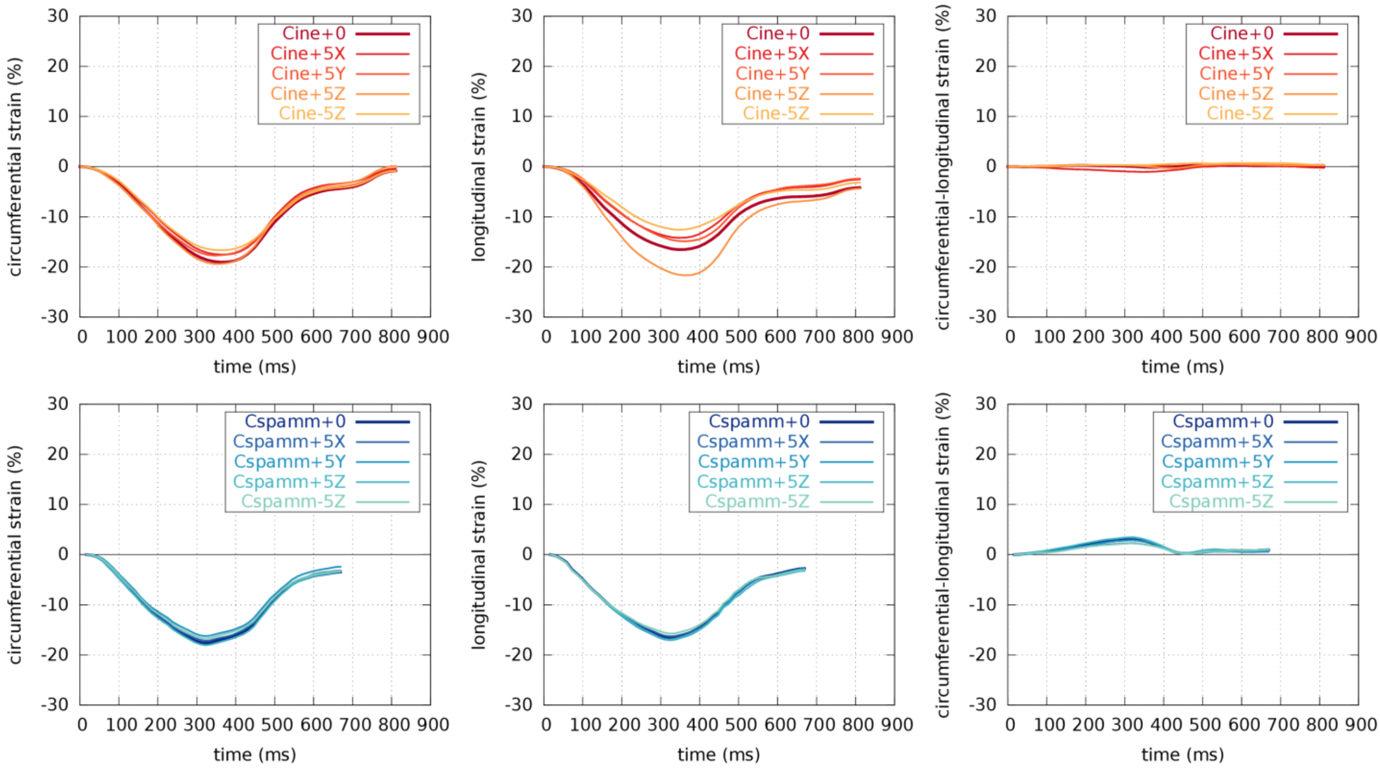

Comparison of time courses of mean circumferential (left), longitudinal (center) and circumferential-longitudinal (right) strain components derived from cine (top) vs. 3D CSPAMM (bottom) images including in-plane (intermediate reds & blues) and out-of-plane (lighter reds & blues) image/mesh misregistration of 5mm.

Synopsis (Max 100 words)

The objective of the present work was to develop, validate and analyze a finite element digital image correlation approach of extracting ventricular strain data from MR images, which can be applied to both 3D CSPAMM images and conventional multi-slice cine images. Cine and 3D CSPAMM data was acquired on a normal human volunteer, and analyzed. The proposed method provided similar circumferential strain data compared to already validated SinMod method. In contrast to strain mapping from cine images, strain mapping from 3D CSPAMM images captures ventricular twist and torsion in agreement with physiological values, and is less sensitive to image misregistration.